Biogeosciences
Discussions

Technical note: Facilitating the use of low-cost methane (CH₄) sensors in flux chambers – calibration, data processing, and an open source make-it-yourself logger

5   David Bastviken[1], Jonatan Nygren[1], Jonathan Schenk[1], Roser Parellada Massana[1], Nguyen Thanh Duc[1]

[1]Department of Thematic Studies – Environmental Change, Linköping University, 58183 Linköping, Sweden
Correspondence to: David Bastviken (david.bastviken@liu.se)

Abstract. A major bottleneck regarding the efforts to better quantify greenhouse gas fluxes, map sources and sinks, and

10   understand flux regulation, is the shortage of low-cost and accurate-enough measurement methods. The studies of methane (CH_4) – a long-lived greenhouse gas increasing rapidly but irregularly in the atmosphere for unclear reasons, and with poorly understood source-sink attribution – suffer from such method limitations. This study present new calibration and data processing approaches for use of a low-cost CH_4 sensor in flux chambers. Results show that the change in relative CH_4 levels can be determined at rather high accuracy in the 2 – 700 ppm range, with modest efforts of collecting reference samples *in*

15   *situ*, and without continuous access to expensive reference instruments. These results open for more affordable and time-effective measurements of CH_4 in flux chambers. To facilitate such measurements, we also provide a description for building and using an Arduino logger for CH_4, carbon dioxide (CO_2), humidity, and temperature.

1 Introduction

Methane (CH_4) is the second most important of the long-lived greenhouse gases (GHGs). Its global 100-year warming

20   potential per mass (GWP_{100}) is 28-34 times greater than the GWP_{100} for carbon dioxide (CO_2), and its relative increase in the atmosphere since 1750 have been much greater than for other GHGs (e.g. Myhre et al., 2013). The atmospheric CH_4 originate from multiple sources including incomplete combustion, natural or biogas gas handling, or microbial CH_4 production in agriculture, ruminant digestive tracts, and other anaerobic environments such as wetlands and lakes – the microbial CH_4 accounting for approximately two thirds of the total emissions (e.g. Saunois et al., 2016). The high diversity

25   of sources, many yielding fluxes that have high spatio-temporal variability, makes it difficult to quantify fluxes and understand flux regulation without a large number of local measurements. At the same time, common methods to measure fluxes rely on expensive equipment or labour-demanding procedures. Consequently, the CH_4 flux from various sources are poorly constrained. This is exemplified by the discovery of inland waters and flooded forests as two large global CH_4 sources during the last decade (Bastviken et al., 2011;Pangala et al., 2017). Greater availability of measurement approaches

30   that are inexpensive enough to allow many measurements and assessment of both spatial and temporal variability simultaneously, would greatly improve our ability to assess landscape CH_4 fluxes and flux regulation.

1

There is extensive work to develop sensitive, small, and affordable CH_4 sensors, but so far the commercially available low-cost CH_4 sensors were typically developed for explosion warning systems and thereby for high concentrations (percent

35 levels). CH_4 detection at such levels is of high interest for environmental research, including the measurements of CH_4 ebullition, and for such applications cost-efficient sensor applications have been presented (e.g. Maher et al., 2019). For measurements of other types of CH_4 fluxes, sensors with robust and reliable detection at lower levels (ppm) are needed. Previous attempts to use and calibrate such sensors at low levels have been promising (e.g. Eugster and Kling, 2012; see Table S2), but also reported remaining challenges, and the use of these sensors in environmental research or monitoring has

40 not yet become widespread. The direct monitoring of atmospheric CH_4 levels to resolve fluxes, demanding fast and accurate detection of changes in the order of 10ppb, still represents a challenge for low-cost sensors. However, relevant level ranges for flux chamber studies (2 – ~1000 ppm depending on environment, chamber type, and deployment times) appear within reach.

45 One commercially available low-cost sensor type, showing promising performance in previous studies, are represented by the TGS 2600 tin dioxide (SnO_2) semiconductor sensor family made by Figaro. This type of sensors has been evaluated multiple times at CH_4 levels near ambient background air (from 1.8 to 9 ppm; different ranges in different studies; Eugster and Kling, 2012; Casey et al., 2019; Collier-Oxandale et al., 2018; van den Bossche et al., 2017). Given their low cost, they performed surprisingly well under non-sulphidic conditions (H_2S may interfere with the sensors), although it was

50 challenging to generate calibration models with $R^2 > 0.8$, and the reported interferences from e.g. relative humidity (RH) and temperature (T) were large (van den Bossche et al., 2017; Table S2). We here evaluate one member of this sensor family for a larger CH_4 range (2-719 ppm), selected to be appropriate for use in automated and manual flux chambers. We propose further development of the equations suggested by the manufacturer for data processing, and provide guidance on how to address the sensor response to humidity (H), RH and T in flux chamber applications. We also describe a simple

55 CH_4/CO_2/RH/T logger based on the evaluated sensors, an Arduino microcontroller, and a corresponding logger shield.

2 Methods

2.1 The CH_4 sensor

The sensor used in this study is the Figaro NGM 2611-E13, which is a factory pre-calibrated module based on the Figaro TGS 2611-E00. The factory calibration is made at 5000 ppm, 20 °C and 65% RH. These levels are is not relevant for

60 applications near atmospheric concentration or variable T and RH, but the NGM 2611-E13 is compact and ready-to-use, facilitating its integration with data loggers and equipment for flux measurements (eg. automated flux chambers; Duc et al., 2013; Thanh Duc et al., 2019). The detection range given by the manufacturer is 500-10000 ppm, but the sensor has been used successfully for measuring indoor ambient concentrations of methane (van den Bossche et al., 2017). The potential of

another similar sensor, the Figaro TGS 2600, for atmospheric concentration monitoring have been investigated (Eugster and
Kling, 2012; Collier-Oxandale et al., 2018). The main difference of the TGS 2611-E00, compared to the TGS 2600, is the
presence of a filter that reduce the interference of other combustible gases with the sensor, making it more selective towards
CH_4 (Figaro_TGS_2611-E00, REV: 10/13). The TGS 2611-E00 is also more than 10 times cheaper than the sensor used in
Duc et al. (2013) and its detection range is wider, allowing for reliable measurements of concentration above 1000 ppm,
which makes the sensor potentially useful in both low- and high-emitting environments.

2.2 Calibration setup

The sensor evaluation set-up was designed to resemble real measurement conditions in floating flux chambers in aquatic
environments. The sensors were placed in the headspace of a plastic bucket positioned upside down on a water surface in a
tank. We used a 7L plastic bucket in which we located 20 TGS 2611-E13 sensors connected to electronic circuitry and
sensor signal logging system described in detail separately (Thanh Duc et al., 2019). The chamber headspace was
continuously pumped from the chamber, through the measurement cell of an Ultraportable Greenhouse Gas Analyzer
(UGGA; Los Gatos Research), and then back to the chamber. The UGGA served as a reference instrument for CH_4. The air
T and RH inside the chamber were measured with ten K33-ELG sensors which have an accuracy of ± 0.4°C and ± 3% RH
(Senseair; also used for CO_2-measurements and therefore suitable for simultaneous use in flux chamber measurements;
Bastviken et al., 2015; data from two K33-ELG sensors and four CH_4 sensors were logged together). The entire installation
was placed in a climate room to allow for varying T, and thereby also absolute humidity (H) in the chamber headspace. T and
H co-vary under field conditions in measurements near moist surfaces, so although T and H were not controlled
independently, their variability under this calibration setup was reflecting flux chamber headspace conditions under in situ
field conditions.

The CH_4 concentration in the chamber was changed by direct injections of methane into the chamber by syringe via a tube.
The CH_4 concentrations during the calibration experiments ranged from 2 ppm to 719 ppm. We performed multiple separate
calibration experiments at different T and RH levels ranging from 10 to 42 °C and 18 – 70 %. Values were recorded once per
minute. T and RH values form the CO_2 sensors were averaged among all sensors before used in the evaluation.

The response time to changing chamber headspace CH_4 levels differed between the sensors situated in the chamber
(responding rapidly), and the UGGA (delayed response time due to the residence time of the measurement cell and tubing).
Therefor data were filtered to remove periods of rapid changes when the different response times caused data offsets. Some
sensor data were lost during parts of the experiments due to power, connection failure, or data communication issues.
Altogether on an average, after data filtration, 619 – 930 data points from each sensor and the UGGA, respectively, were
used for the evaluation (in total 20 CH_4 sensors evaluated).

2.2 Data processing and interpretation

The TGS 2611 SnO_2 sensing area exhibit decreasing resistance with increasing methane concentration (Figaro_Tech_Info_TGS2611, 2012). The sensing area is connected in series with a reference resistor (resistance referred to as R_L). The total circuit voltage (V_C) is 5V across both the sensing area and the reference resistor. The voltage across the

100   reference resistor (V_L) therefore varies in response to how the sensing area resistance (R_S) varies. V_L is measured and reported as output voltage. The sensor response R_S is calculated from the following equation (Figaro_Tech_Info_TGS2611, 2012; Figaro_TGS_2611-E00, REV: 10/13):

$$R_s = \left(\frac{V_C}{V_L} - 1\right) \times R_L \tag{1}$$

105

The active sensor surface characteristics and R_L can differ among individual sensors, which makes individual sensor calibration necessary. Interference by water vapour and T has been previously shown (Pavelko, 2012; van den Bossche et al., 2017). R_L is therefore ideally determined in dry air containing no volatile organic compounds or other reduced gases at a standard T. However, it can be challenging to determine R_L, and Eugster and Kling (2012) proposed to use the lowest

110   measured sensor output voltage (V_0), representing minimum background atmospheric levels, to determine an empirical reference resistance R_0, and to calculate the ratio of R_S/R_0, reflecting the relative sensor response as follows:

$$\frac{R_S}{R_0} = \frac{\left(\frac{V_C}{V_L} - 1\right)}{\left(\frac{V_C}{V_0} - 1\right)} \tag{2}$$

115   This approach allows sensor use without accurate specific determination of R_L. Previous attempts to calibrate these type of sensors for environmentally relevant applications have focused on CH_4 levels of 2-9 ppm, and typically considered the influence of T and RH or H (Casey et al., 2019; van den Bossche et al., 2017; Collier-Oxandale et al., 2018; Eugster and Kling, 2012). In these cases, an approximately linear response of the relative sensor response could be assumed due to the narrow CH_4 range. However, the sensor response is non-linear in the range relevant for flux chamber measurements and in

120   this wider range, other approaches are needed. We here present a two-step sensor calibration based on the complete calibration experiment data. In addition, we tried simplified calibration approaches for situations when full calibration experiments are not feasible and when access to reference instruments is limited. These approaches are described below.

2.2.1 Two-step calibration from complete experimental data (Approach I)

The first step (Step1) regards determination of the reference sensor resistance, R_0. We assumed that R_0 represented R_L +

125   R_{Sbkg}, where R_{Sbkg} is R_S at the background atmospheric CH_4 level. We first tried the previously suggested approach to determine R_0 from the minimum V_L, i.e. setting V_0 to V_L at the lowest humidity and CH_4 concentrations during all

measurements, thereby assuming that R_0 could be seen as constant. However, R_{Sbkg} may be influenced by H and T and could vary even if the CH_4 levels at background atmospheric conditions are constant. Thus, we also tested ways to correct R_0 to RH or H and T. Therefore, after selecting the experiment data at background CH_4 levels but variable humidity and temperature,

130   we tested linear, power, or Michaelis-Menten models, to generate V_0 values valid for different humidity and temperatures. This allowed estimation of R_0 values at the humidity and temperature associated with each R_S value, making the R_S/R_0 ratio less biased. The background level CH_4 data was selected in two different ways – either as all known CH_4 values below 2.5 ppm (n = 38-72), or as the minimum V_L value for each experiment and sensor (n = 6-7).

135   The second step (Step 2) regards calculation of CH_4 levels from R_S/R_0. Several models were tested, where the CH_4 levels were estimated as a function of R_S/R_0, humidity, temperature, and a constant to consider offsets that may differ among sensors. We tried several linear and power functions. In line with viewing the sensor surface as an active site where CH_4 and H_2O compete for space, the humidity effect was in some models represented as an interaction with the sensor response. In all above cases, models were generated by curve-fitting in Python using the scipy.optimize curve_fit function. Predicted

140   CH_4 levels were evaluated by comparison with the observed levels (independently measured by the UGGA). The specific model equations are provided in Table 1 and 2. We tested models using RH or H (which was calculated from RH and T; (Vaisala_Technical_Report, 2013). Each evaluation included a combination of both steps above, and generated one set of fitted parameters per sensor used, including the parameters for Step 1 and 2.

2.2.2 Simplified calibration approaches without dedicated calibration experiment data (Approach II and III)

145   The model combinations from Step 1 and 2 above that generated the best fit with the minimum number of parameters was selected for tests of two simplified calibration approaches. In *Approach II* we tested if model parameters in Step 2 can be predicted from parameters derived in Step 1, hypothesising that the derived model parameters in both Step 1 and Step 2 reflect the sensor capacity to respond to CH_4 and humidity levels as well as the individual sensor offset. If correct, the parameters in Step 1 should be correlated with parameters in Step 2. If this correlation is strong enough, it may be possible to

150   predict parameters in Step 2 from parameters in Step 1, which can be derived from measurements at background air concentrations under the natural variation in humidity (e.g. the diel variability), as a part of the regular measurements, preferentially using data when the atmospheric boundary layer is well mixed (e.g. windy conditions). Under such conditions atmospheric background CH_4 concentrations can be relatively accurately assumed. Hence this Approach II would not require access to sensor calibration chambers nor expensive reference gas analysers, which in turn would make sensor measurements

155   available much more broadly. To test this approach, we searched for the best possible regression equations to predict Step 2 parameters from Step 1 parameters, then used these equations to estimate CH_4 levels, and compared estimated levels versus observed.

In *Approach III* we evaluated if reasonable accurate Step 1 and 2 equations can be derived from the combination of (*i*)
160 minimum background atmospheric level V_L at different humidity, and (*ii*) a limited number of randomly collected
independent manual flux chamber samples. If so, a few manual samples during the regular measurements could replace
tedious dedicated calibration experiments. To test this approach the calibration data for each sensor was subsampled
randomly and this random subset data were combined with the minimum V_L data to derive calibration parameters as done in
Approach I. Using these parameters, the CH_4 levels for the entire calibration data was estimated and compared with observed
165 values. Monte Carlo simulations were run to test effects of the number of random reference samples (1 – 50) and the
methane concentration ranges (3 – 500 ppm, or 3-50 ppm, respectively) in the subset data.

2.2.3 A low-cost Arduino-based CH₄/CO₂/*RH*/*T* logger

To facilitate use of the sensors and our results, we also gathered instructions for how to build a logger for CH_4, CO_2, *RH* and
T measurements, using the CH_4 sensor tested here, and the Senseair K33 ELG CO_2/*RH*/*T* sensor described elsewhere
170 (Bastviken et al., 2015), a supplementary DHT22 sensor for *RH* and *T*, an Arduino controller unit, and an Adafruit Arduino
compatible logger shield with a real time clock (Figure 2). This development was based on sensor specifications and the
open source knowledge generously shared on internet by the Arduino user community. The full description of this logger
unit is found in the Supplement.

3 Results and Discussion

175 The results of different Step 1 and Step 2 calibration equations are shown in Tables 1 and 2. The models including *H* were
equal or superior to models using *RH*. This is reasonable because it is the absolute water molecule abundance that influence
the sensor response. Hence, models using *H* were prioritized. In *Approach I*, several Step 1 models, including a constant
minimum V_L, and power, linear and Michaelis-Menten-based equations gave similar R^2 (0.85 to 0.9) and root mean square
error (RMSE) when comparing predicted versus observed results (Table 1). The effect of *T* appeared negligible compared to
180 *H*, which may be related to the built-in heating of the active sensor surface. It is possible that the Michaelis-Menten equation
is superior over the full theoretically possible *H* range. However, under our experiment conditions, covering normal field *H*
levels, the combination of best fit and minimum number of parameters in Step 1, was found for a simple linear equation with
H (Model V4 in Table 1), which was used for later tests of *Approach II* and *III*.

185 The tests of different equations in Approach I, Step 2, showed that power relationships with *H* and *T* represented as
interactions with the sensor response, performed best (Table 2 Model ≥4). With the exception of Models 10a-c, all these
models had in the regression of observed versus predicted, a slope and intercept that was statistically indistinguishable from
1 and 0, respectively ($p < 0.05$) and an R^2 of 0.98 – 1.00 (Table 2, Figure S1). Again, *T* had a marginal effect and *H* was
clearly most important. Hence, while Model 7 including *T* in Table 2 had the lowest RMSE (9.8), Model 8 represented a

190   good compromise between minimum number of parameters and low RMSE (10.4) and was used in Approach II and III. The non-linear response of the sensor yielded a stronger and more coherent response at low CH_4 levels, and a large part of the uncertainty were generated at the higher CH_4 levels in the studied range (Figure S1). Near the atmospheric background at 2 ppm, the confidence interval for individual sensor response was in the order of $\pm$ 1.1 ppm (Model 7 having lowes RMSE). Hence, the presented calibration equations have a limited accuracy in terms of absolute CH_4 levels, and is not optimized for

195   high-precision measurements at atmospheric background levels. However, results indicate that the relative change of CH_4 levels over time, which is the core of flux chamber measurements, can be assessed efficiently with the sensors if calibrated properly.

Approach II, deriving all calibration equations from a small set of minimum V_L values using Models V4 or V5 (Table 1) and

200   10a-c (Table 2), generated substantially greater RMSE. Most of this RMSE change was due to less accurate prediction of the intercept. The R^2 and slope standard error range remained similar to the other models (Table 2), but the actual slope values could deviate substantially from 1 and varied considerably among sensors (in contrast to the models for all other approaches always having slopes close to 1 and similar among sensors; Figure S1). Thereby, Approach II could lead to a large bias in absolute levels, and this crude generation of calibration equations may be adequate primarily for assessing relative change

205   over time measured by the same sensor, and cross comparisons among sensors should be avoided when using this approach. Examples of equations for the parameter estimation in Approach II is provided in Table S1. Applying Approach II on a smaller concentration range yielded a considerably lower RMSE (Table 2, Model 10c).

Approach III (Model 11a and 11b in Table 2) showed that as few as 20 reference samples, collected at random occasions

210   during actual measurements, could substantially reduce the RMSE of the calibration models, reaching close to the lowest levels based on the 619 – 930 measurements and the full range up to 719 ppm in Approach I (Table 2 Model 11a; Figure S2). The concentrations of the reference samples did not appear important for the RMSE within a given specific data range. However, simulations using data for CH_4 levels below 50 ppm only, generated much lower RMSE than using all data (Table 2, Model 11b). This support the conclusion that the sensors are more sensitive and give a stronger relative response in the

215   low part of the studied concentration range.

An overview of approaches to derive calibration models for this type is shown in Table S2. The challenges found regarding monitoring of background atmospheric levels was confirmed by our study, while use for relative changes of greater magnitudes in flux chambers appear promising based on this study, also with a simplified calibration (Approach III).

220   **4 Conclusions**

The main conclusions can be summarized by the following:

- The tested CH$_4$ sensors are suitable for use in flux chamber applications if there are simultaneous measurements of relative humidity and temperature (or humidity).

- Sensor-specific calibration is required.

225
- Occasional independent reference samples during regular measurements, is an alternative to designated calibration experiments. Background atmospheric levels in combination in the order of 20 *in situ* reference samples at other CH$_4$ levels, can yield rather accurate calibration models.

- For highest accuracy regarding absolute CH$_4$ concentrations, careful designated calibration experiments covering relevant environmental conditions are needed.

230
- These results, together with the increased accessibility of low-cost sensors and data logger systems (one example described in the Supplement), open supplementary paths toward improved capacity for greenhouse gas measurements in both nature and society.

5 Code and data availability

Python code for data evaluation and the calibration experiment data is available from the main author upon request. Please
235 note that both the code and the data are specific for the experimental setup. The Python code needs modifications for use with other data, and the CH$_4$ sensor data cannot represent results from other sensors as sensor specific calibration is needed. The Arduino code for the CH$_4$/CO$_2$/*RH*/*T* logger described in the supplement is available at http://urn.kb.se/resolve?urn=urn:nbn:se:liu:diva-162780.

240 ## 6 Author contribution

DB and NTD designed and supervised the study. NTD designed and built the experimental setup, the sensor units and the data logging system. JN and NTD performed the calibration experiment. The analysis of the sensor data was led by DB with contributions from NTD, JS, and JN. DB and NTD developed the logger units presented in the supplementary material. RP helped to build and test logger units and drafted a user manual. DB wrote the first complete draft of the manuscript and led
245 the manuscript development, with contributions from NTD, JS, RP, and JN.

7 Competing interests

There are no competing interests.

Biogeosciences
Discussions

Open Access

EGU

References

255   Bastviken, D., Tranvik, L. J., Downing, J. A., Crill, P. M., and Enrich-Prast, A.: Freshwater methane emissions offset the continental carbon sink, Science, 331, doi.org/10.1126/science.1196808, 2011.

Bastviken, D., Sundgren, I., Natchimuthu, S., Reyier, H., and Gålfalk, M.: Technical Note: Cost-efficient approaches to measure carbon dioxide (CO_2) fluxes and concentrations in terrestrial and aquatic environments using mini loggers,
260   Biogeosciences, 12, 3849–3859, doi.org/10.5194/bg-12-3849-2015, 2015.

Casey, J. G., Collier-Oxandale, A., and Hannigan, M.: Performance of artificial neural networks and linear models to quantify 4 trace gas species in an oil and gas production region with low-cost sensors, Sensors and Actuators B: Chemical, 283, 504-514, doi.org/10.1016/j.snb.2018.12.049, 2019.
265

Collier-Oxandale, A., Casey, J. G., Piedrahita, R., Ortega, J., Halliday, H., Johnston, J., and Hannigan, M. P.: Assessing a low-cost methane sensor quantification system for use in complex rural and urban environments, Atmos. Meas. Tech., 11, 3569-3594, doi.org/10.5194/amt-11-3569-2018, 2018.

270   Duc, N. T., Silverstein, S., Lundmark, L., Reyier, H., Crill, P., and Bastviken, D.: An automated flux chamber for investigating gas flux at water – air interfaces, Environ. Sci. Technol., 47 968–975, doi.org/10.1021/es303848x, 2013.

Eugster, W., and Kling, G. W.: Performance of a low-cost methane sensor for ambient concentration measurements in preliminary studies, Atmospheric Measurement Techniques, 5, 1925-1934, doi.org/10.5194/amt-5-1925-2012, 2012.
275

Figaro_Tech_Info_TGS2611: Technical information for TGS2611, http://www.figarosensor.com/products/2611Dtl.pdf, 2012.

Product information TGS 2611-E00, REV: 10/13, www.figarosensor.com/product/docs/TGS%202611C00(1013).pdf, 2013

280

Maher, D. T., Drexl, M., Tait, D. R., Johnston, S. G., and Jeffrey, L. C.: iAMES: An inexpensive, Automated Methane Ebullition Sensor, Environmental Science & Technology, 53, 6420-6426, doi.org/10.1021/acs.est.9b01881, 2019.

Myhre, G., Shindell, D., Bréon, F.-M., Collins, W., Fuglestvedt, J., Huang, J., Koch, D., Lamarque, J.-F., Lee, D., Mendoza, 285 B., Nakajima, T., Robock, A., Stephens, G., Takemura, T., and Zhang, H.: Anthropogenic and Natural Radiative Forcing, in: Climate Change 2013: The Physical Science Basis. Contribution of Working Group I to the Fifth Assessment Report of the Intergovernmental Panel on Climate Change, edited by: Stocker, T., Qin, D., Plattner, G.-K., Tignor, M., Allen, S., Boschung, J., Nauels, A., Xia, Y., Bex, V., and Midgley, P., Cambridge University Press, Cambridge, United Kingdom and New York, NY, USA, 2013.

290

Pangala, S. R., Enrich-Prast, A., Basso, L. S., Peixoto, R. B., Bastviken, D., Hornibrook, E. R. C., Gatti, L. V., Marotta, H., Calazans, L. S. B., Sakuragui, C. M., Bastos, W. R., Malm, O., Gloor, E., Miller, J. B., and Gauci, V.: Large emissions from floodplain trees close the Amazon methane budget, Nature, 552, 230, doi.org/10.1038/nature24639 https://www.nature.com/articles/nature24639#supplementary-information, 2017.

295

Pavelko, R.: The influence of water vapor on the gas-sensing phenomenon of tin dioxide–based gas sensors, in: Chemical Sensors: Simulation and Modeling Volume 2: Conductometric-Type Sensors, edited by: Korotcenkov, G., Momentum Press, New York, 297-330, 2012.

300 Saunois, M., Bousquet, P., Poulter, B., Peregon, A., Ciais, P., Canadell, J. G., Dlugokencky, E. J., Etiope, G., Bastviken, D., Houweling, S., Janssens-Maenhout, G., Tubiello, F. N., Castaldi, S., Jackson, R. B., Alexe, M., Arora, V. K., Beerling, D. J., Bergamaschi, P., Blake, D. R., Brailsford, G., Brovkin, V., Bruhwiler, L., Crevoisier, C., Crill, P., Covey, K., Curry, C., Frankenberg, C., Gedney, N., Höglund-Isaksson, L., Ishizawa, M., Ito, A., Joos, F., Kim, H. S., Kleinen, T., Krummel, P., Lamarque, J. F., Langenfelds, R., Locatelli, R., Machida, T., Maksyutov, S., McDonald, K. C., Marshall, J., Melton, J. R., 305 Morino, I., Naik, V., O'Doherty, S., Parmentier, F. J. W., Patra, P. K., Peng, C., Peng, S., Peters, G. P., Pison, I., Prigent, C., Prinn, R., Ramonet, M., Riley, W. J., Saito, M., Santini, M., Schroeder, R., Simpson, I. J., Spahni, R., Steele, P., Takizawa, A., Thornton, B. F., Tian, H., Tohjima, Y., Viovy, N., Voulgarakis, A., van Weele, M., van der Werf, G. R., Weiss, R., Wiedinmyer, C., Wilton, D. J., Wiltshire, A., Worthy, D., Wunch, D., Xu, X., Yoshida, Y., Zhang, B., Zhang, Z., and Zhu, Q.: The global methane budget 2000–2012, Earth Syst. Sci. Data, 8, 697-751, 10.5194/essd-8-697-2016, 2016.

310

Thanh Duc, N., Silverstein, S., Wik, M., Crill, P., Bastviken, D., and Varner, R. K.: Greenhouse gas flux studies: An automated online system for gas emission measurements in aquatic environments, Hydrol. Earth Syst. Sci. Discuss., 2019, 1-18, 10.5194/hess-2019-83, 2019.

315   Vaisala_Technical_Report: Humidity conversion Formulas. Calculation fromulas for humidity., Finland, 17, https://www.hatchability.com/Vaisala.pdf, 2013.

        van den Bossche, M., Rose, N. T., and De Wekker, S. F. J.: Potential of a low-cost gas sensor for atmospheric methane

320   monitoring, Sensors and Actuators B: Chemical, 238, 501-509, https://doi.org/10.1016/j.snb.2016.07.092, 2017.

Table 1: Model results for Step 1 of sensor calibration - i.e. the correction of reference output voltage (V_0 in the unit mV) in background
325 air to humidity and temperature. V_{0min}, H, and T, represent the minimum V_0 for each sensor (mV), absolute humidity (ppm), and
temperature (°C) during measurements in open air. The model parameters g, h, S, m and n are constants for each sensor derived by curve
fitting. The model R^2 is the adjusted coefficient of determination (mean, minimum and maximum for the 20 sensors tested), and RMSE is
then root mean square error. Equivalent models using relative humidity (RH; %) instead of H, returned lower R^2 and higher RMSE and are
not shown. These Step 1 models were combined with the Step 2 models as noted in Table 2. See text for details.

| **Model for V_0**		**Data**	**n**	**Observed vs. Predicted**			
No.	**Equation**			R^2			**RMSE**
				mean	min	max	mean
V1	V_{0min} (constant)	Minimum V_0	1	-	-	-	-
V2	$V_0 = gH^h + mT^n + S$	All < 2.5 ppm CH$_4$	38 - 72	0.85	0.66	0.94	8.9
V3	$V_0 = gH + mT + S$	All < 2.5 ppm CH$_4$	38 - 72	0.88	0.68	0.95	8.2
V4a	$V_0 = gH + S$	All < 2.5 ppm CH$_4$	38 - 72	0.88	0.68	0.95	8.2
V4b	$V_0 = gH + S$	Min V_0 for each exp.	6 - 7	0.90	0.72	0.96	8.3
V5a	$V_0 = gH / (S + H)$	All < 2.5 ppm CH$_4$	38 - 72	0.88	0.70	0.96	8.0
V5b	$V_0 = gH / (S + H)$	Min V_0 for each exp.	6 - 7	0.89	0.71	0.96	8.3

330

Table 2: Model results for Step 2 of the data evaluation, i.e. the determination of methane (CH_4) levels (ppm) from the sensor response expressed as R (corresponding to R_S/R_0) using different calibration models. (RH), H, and T as defined in Table 1. The model parameters a, b, c, d, e, f and K are constants for each sensor derived by curve fitting. The models were evaluated via a linear regression of *Observed* versus *Predicted* CH_4 levels, where k and M are the slope and the intercept, respectively. SE denote standard error, R^2 the adjusted coefficient of determination (mean and minimum to maximum for the 20 sensors tested), and RMSE is the root mean square error. The table show the most successful subset of all models tested. N = 619 – 930 per sensor in total and 203-313 for the data subset with CH4 levels < 50 ppm. See text for details.

Model No.	Equation	V_0 mod	CH_4 max ppm	k SE (min-max)	M min to max*	SE (min-max)	R^2 mean (min-max)	RMSE mean (min-max)
					Observed $= k * Predicted + M$			
1	$CH_4 = aR + b(RH) + cT + K$	V1	719	0.024-0.036	$-3.2 \cdot 10^{-7}$ to $3.5 \cdot 10^{-7}$	5.8-8.2	0.58 (0.54-0.68)	117 (104-127)
2	$CH_4 = aR^b + c(RH)^d + eT^f + K$	V1	719	0.006-0.010	$-8.8 \cdot 10^{-7}$ to $4.2 \cdot 10^{-7}$	1.6-2.6	0.96 (0.94-0.97)	35.9 (32-45)
3	$CH_4 = aR^b + c(RH)(aR^b) + dT(aR^b) + K$	V1	719	0.003-0.006	$-6.8 \cdot 10^{-7}$ to $9.3 \cdot 10^{-7}$	0.72-1.44	0.99 (0.98-0.99)	18.5 (15-25)
4	$CH_4 = aR^b + cH(aR^b) + dT(aR^b) + K$	V1	719	0.002-0.003	$-4.3 \cdot 10^{-7}$ to $3.2 \cdot 10^{-7}$	0.43-0.90	1.00 (0.99-1.00)	11.4 (9-16)
5	As No. 4	V2	719	0.001-0.003	$-3.3 \cdot 10^{-7}$ to $4.1 \cdot 10^{-7}$	0.38-0.87	1.00 (0.99-1.00)	10.6 (8-16)
6	As No. 4	V3	719	0.001-0.003	$-4.1 \cdot 10^{-7}$ to $3.6 \cdot 10^{-7}$	0.37-0.82	1.00 (0.99-1.00)	9.8 (8-15)
7	As No. 4	V4a	719	0.001-0.003	$-2.2 \cdot 10^{-7}$ to $2.8 \cdot 10^{-7}$	0.37-0.82	0.99 (0.99-1.00)	9.8 (8-14)
8	$CH_4 = aR^b + cH(aR^b) + K$	V4a	719	0.001-0.003	$-5.6 \cdot 10^{-7}$ to $1.3 \cdot 10^{-7}$	0.37-0.84	1.00 (0.99-1.00)	10.4 (8-15)
9a	As No. 8 with equation V4b to determine V0.	V4b	719	0.001-0.003	$-7.8 \cdot 10^{-7}$ to $1.4 \cdot 10^{-6}$	0.37-0.84	1.00 (0.99-1.00)	10.4 (8-15)
9b	As No. 9a with lower max CH4 level.	V4b	50	0.007-0.014	$-4.1 \cdot 10^{-8}$ to $8.1 \cdot 10^{-8}$	0.16-0.33	0.98 (0.96-0.99)	2.1 (2-3)

| No	Description							
10a	As No 8. Parameters a, b, c and K estimated from relationships with parameters in V4b; see text.	V4b	719	0.001-0.012	-108 to 1.1	0.39-1.62	1.00 (0.99-1.00)	74 (18-150)
10b	As No 8. Parameters a, b, c and K estimated from relationships with parameters in V5b; see text.	V5b	719	0.001-0.024	-122 to 1.9	0.43-2.80	0.99 (0.96-1.00)	88 (20-154)
10c	As No. 10a with lower max CH_4 level.	V4b	50	0.006-0.021	-51 to -14	0.30-0.87	0.98 (0.96-0.98	28 (21-35)
11a	As No. 8. Parameters a, b, c, and K, *derived* from 6-7 minimum V_L values at different H, and 20 samples at random CH_4 levels between 3 and 500 ppm.**	V4b	719	0.002-0.004	-6.5 to 7.1	0.41-0.96	1.00 (0.99-1.00)	13 (8.8-20)
11b	As No. 11a with the 20 random samples at CH_4 levels between 3 and 50 ppm.**	V4b	50	0.008-0.017	-0.7 to 0.5	0.17-0.41	0.97 (0.95-0.98)	2.5 (2-3)

*Minimum and maximum mean intercepts for the group of 20 sensors. The confidence interval around the mean intercept was ± 1.1 ppm in Model 7 (having lowest RMSE). ** Monte Carlo simulations with 1000 runs generating random data subsets used for deriving the model parameter ranges.

345
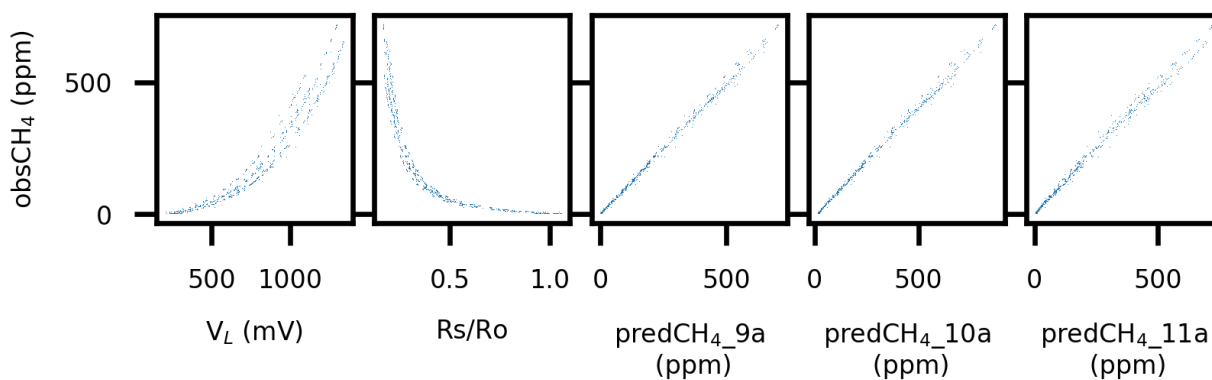
Figure 1. Sensor output voltage (V_L; mV), Rs/R_0 ratio, and predicted CH_4 mixing ratio (predCH4; ppm) using Model 9a, 10a and 11a in Table 2, respectively, versus observed CH_4 mixing ratio (obsCH4; ppm), for one of the studied sensors. See text for details and Figure S1 for similar graphs regarding all sensors.
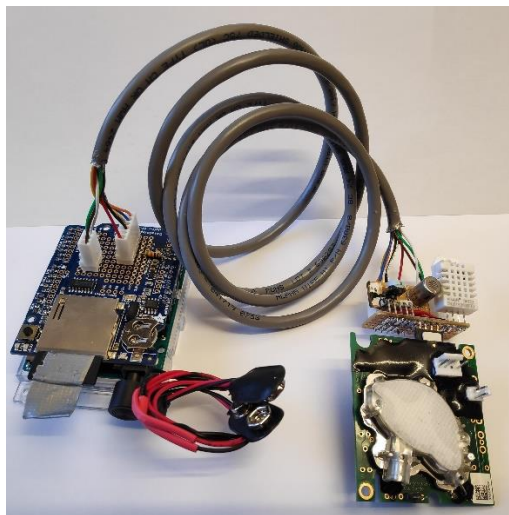
355

Figure 2. Photo of the CH$_4$/CO$_2$/RH/T logger described in the supplementary information.